Contrast-enhanced ultrasound molecular imaging of activated platelets in the progression of atherosclerosis using microbubbles bearing the von Willebrand factor A1 domain

JIE TIAN, YAHUI WENG, RUIYING SUN, YING ZHU, JUN ZHANG, HONGYUN LIU and YANI LIU

Department of Medical Ultrasound, Tongji Hospital, Tongji Medical College, Huazhong University of Science and Technology, Wuhan, Hubei 430030, P.R. China

Received January 21, 2020; Accepted March 15, 2021

DOI: 10.3892/etm.2021.10153

Abstract. Platelet-endothelial interactions have been linked to increased inflammatory activation and a prothrombotic state in atherosclerosis. The interaction between von Willebrand factor (vWF)-A1 domain and platelet glycoprotein (GP) Ib/IX plays a significant role in mediating the adhesion of platelets to the injured endothelium. In the present study, contrast-enhanced ultrasound (CEU) molecular imaging with microbubbles bearing the vWF-A1 domain was performed to non-invasively monitor activated platelets on the vascular endothelium in the procession of atherosclerosis. A targeted CEU contrast agent was prepared by attaching the vWF-A1 domain to the shell of microbubbles (Mb_{A1}). Rat isotype control antibody was used to produce control (Mb_{ctrl}) microbubbles. The binding of Mb_{A1} and Mb_{ctrl} to activated platelets was assessed in *in vitro* flow chamber experiments. Apolipoprotein E ($ApoE^{-/-}$) deficient mice were studied as a model of atherosclerosis. At 8, 16 and 32 weeks of age, CEU molecular imaging of the proximal aorta with Mb_{A1} and Mb_{ctrl} was performed and the imaging signals from microbubbles were quantified. Atherosclerotic lesion severity and platelets on the endothelial surface were assessed by histology and immunohistochemistry. In *in vitro* flow chamber studies, attachment of Mb_{A1} to activated platelets on culture dishes was significantly greater than that of Mb_{ctrl} across a range of shear stresses ($P<0.05$). The attachment of Mb_{ctrl} was sparse and not related to the aggregated platelets. As lesion development progressed in the $ApoE^{-/-}$ mice, molecular imaging of activated platelets demonstrated selective signal enhancement of Mb_{A1} ($P<0.05$ vs. Mb_{ctrl}) at all ages. Selective signal enhancement from Mb_{A1} increased from 8 to 32 weeks of age. Immunohistochemistry for GPIIb revealed the presence of platelets on the endothelial cell surface in each group of $ApoE^{-/-}$ mice and that the degree of platelet deposits was age-dependent. The results of the present study indicated that non-invasive CEU molecular imaging with targeted microbubbles bearing the vWF-A1 domain could not only detect activated platelets on the vascular endothelium but also indicate lesion severity in atherosclerosis.

Correspondence to: Dr Yani Liu, Department of Medical Ultrasound, Tongji Hospital, Tongji Medical College, Huazhong University of Science and Technology, 1095 Jiefang Road, Wuhan, Hubei 430030, P.R. China
E-mail: yani.liu@aliyun.com

Key words: atherosclerosis, platelets, platelet glycoprotein Ib, von Willebrand factor A1 domain, targeted microbubbles

Introduction

It is now well established that platelet-endothelial interactions not only contribute to atherogenesis in the late stage of atherosclerosis (AS), which is characterized by plaque destabilization and thrombus formation, but also participate in earlier stages of plaque development, through platelet-mediated inflammatory pathways (1). Although a growing body of literature indicates that contrast-enhanced ultrasound (CEU) with targeted microbubbles allows for the detection of molecular and cellular events related to AS inflammation and plaque vulnerability (2), few studies have been performed to explore the role of activated platelets in the procession of AS.

At sites of vascular injury, the initial adhesion of platelets to the endothelium is mediated through interaction between the glycoprotein-Ibα (GPIbα) subunit of the platelet GPIb-IX-V complex and von Willebrand factor (vWF) (3). After binding to exposed subendothelial collagen, vWF multimers undergo conformational change with exposure of the A1 binding domain to GPIbα. This is regarded as the primary adhesive mechanism, helping the platelet attach itself to the target endothelium in the situation of high shear stress generated by blood flow (4,5).

As the binding of the vWF-A1 domain to the platelet GPIbα receptor is the primary adhesive mechanism for platelet-endothelial interactions (6), it was hypothesized that a recombinant protein with an amino acid sequence corresponding to the vWF-A1 domain would be an ideal target ligand in the preparation of targeted microbubbles to activated platelets. In the present study, targeted CEU microbubbles bearing the recombinant vWF-A1 domain were prepared and their use to image platelets-endothelium interaction and assess platelet-mediated inflammation were assessed in flow-chamber experiments and in a murine model of AS.

Materials and methods

Microbubble preparation. Targeted microbubbles were prepared by surface conjugation of biotinylated ligands, as previously described, using a streptavidin bridge (7). Soluble recombinant vWF-A1 domain (amino acids 1238-1481; U-Protein Express BV) was biotinylated at its N terminus for conjugation to the microbubble shell. For this purpose, a molar excess of EZ-Link™ NHS-Biotin (Thermo Fisher Scientific, Inc.) was reacted overnight at 4˚C with the recombinant vWF-A1 domain in phosphate-buffered saline (PBS, pH 8.0). The resulting bioconjugate was purified using Slide-A-Lyzer Dialysis Cassettes (Thermo Fisher Scientific, Inc.) according to the manufacturer's instructions. The concentration of the recombinant vWF-A1 domain was determined using an automatic amino acid analyzer (model no. L8900; Hitachi, Ltd.) according to the manufacturer's instructions.

Biotinylated, lipid-shelled decafluorobutane microbubbles were prepared by sonication of a gas-saturated aqueous suspension of distearoylphosphatidylcholine (Avanti Polar Lipids, Inc.), polyoxyethylene-40-stearate (Sigma-Aldrich; Merck KGaA) and distearoylphosphatidylethanolamine-PEG (2000) biotin (Avanti Polar Lipids, Inc.). The size and concentration were assessed by an electrozone sensing cell counter (Multisizer III; Beckman-Coulter,Inc.). Control microbubbles (Mb_{ctrl}) were prepared by conjugating biotinylated rat IgG (cat. no. 553880; κ isotype control antibody; BD Biosciences) to microbubbles. Microbubbles targeted to platelets GPIbα (Mb_{A1}) were prepared by conjugating biotinylated vWF-A1 to the shell surface. As described in a previous study (8), biotinylated ligands in excess amounts (50 μg per $1x10^8$ microbubbles) were added to occupy all binding sites on the shell of the microbubbles.

In *in vitro* flow chamber studies, Mb_{A1} and Mb_{ctrl} were labeled with dioctadecyloxacarbocyanine (DiO) and dioctadecyltetramethylindocarbocyanine (DiI) perchlorate (Sigma-Aldrich; Merck KGaA), separately.

Flow chamber activated platelets attachment studies

Preparation of platelet-rich plasma. Blood samples were obtained from 20 random healthy human volunteers (age range, 20-50 years; mean age, 35±10 years; 11 males; 9 females) at the Department of Ultrasound, Tongji Hospital from March 2015 to May 2015. A standardized technique of double centrifugation (9) was used to prepare platelet-rich plasma (PRP). Automatic hemocyte analyzer (model no. XS-800i; Sysmex Corporation) was used to count platelets in PRP. The platelet recovery rate was the total amount of platelets obtained in PRP compared to the number in whole blood. PRP smears were stained with Wright Giemsa (10) to reveal the purity of platelet suspensions. The present study was approved by Tongji Hospital Ethics Committee and written informed consent was obtained from all volunteers before the study.

Coating and activation of platelets. Parallel plate culture dishes with a diameter of 35 mm were incubated with collagen type I (100 μg/ml; Beijing Solarbio Science & Technology Co., Ltd.) at 4˚C overnight and then blocked with bovine serum albumin (5 mg/ml; Wuhan Servicebio Technology Co., Ltd.) at room temperature for 1 h. PRP (platelet concentration, $46x10^6$/ml) and platelet activator was added and incubated at room temperature for at least 15 min. To prepare the platelet activator, 1 ml of 10% calcium chloride was mixed with 500 U of bovine thrombin (Beijing Solarbio Science & Technology Co., Ltd). Indirect immunofluorescence was performed using a rat monoclonal primary antibody against mouse P-selectin (cat. no. CD62P; BD Biosciences) and goat anti-rat Alexa Fluor 488 secondary antibody (Invitrogen; Thermo Fisher Scientific, Inc.) to identify activated platelets.

Flow chamber studies. *In vitro* flow chamber studies were performed at room temperature without specific CO_2 conditions to test the binding of microbubbles to activated platelets under different flow conditions. The parallel plate culture dishes coated with activated platelets were mounted on a parallel plate flow chamber (GlycoTech Corporation) with a gasket thickness of 0.01 in and a channel width of 2.5 mm. To maintain the consistency of the activated platelets on culture dishes, PRP of the same concentration ($46x10^6$/ml) was used in each condition. An aqueous suspension of Mb_{A1} labeled with DiO ($6x10^6$/ml) or Mb_{ctrl} labeled with DiI ($6x10^6$/ml) was drawn through the flow chamber with an adjustable withdrawal pump to generate a flow shear stress of 2.0, 4.0, 6.0 or 8.0 dynes/cm^2, respectively. After 5 min of continuous infusion, freely circulating microbubbles in the chamber were removed by a 2 min PBS rinse at a low shear stress of 0.1 dynes/cm^2. The number of microbubbles adhered to platelets were averaged from 10-15 randomly selected nonoverlapping optical fields under a fluorescent microscope with a 40x objective. Experiments were performed at least in triplicate for each condition.

CEU molecular imaging

Animal models. The study was approved by the Animal Care and Use Committee of Tongji Medical College, Huazhong University of Science and Technology. A total of 20 male wild-type C57Bl/6 mice and 31 apolipoprotein E deficient ($ApoE^{-/-}$) mice with age-dependent atherosclerosis produced on a C57Bl/6 background were studied at 8, 16 and 32 weeks of age (n=8-12 for each strain at each age; Beijing Vital River Laboratory Animal Technology Co., Ltd.). Upon purchase, the mice were 4 weeks of age and weighed ~9 g. As a control, C57Bl/6 mice were fed on a chow diet and from 5 weeks of age onwards, while $ApoE^{-/-}$ mice were fed on a hypercholesterolemic diet (HCD) containing 21% fat by weight, 0.15% cholesterol, and 19.5% casein without sodium cholate. All mice were fed with free food and water access, and were raised in the Animal Experimental Center of Tongji Medical College, Huazhong University of Science and Technology, which had a specifical pathogen free barrier environment. Animals were housed at a temperature of 20-26˚C and a relative humidity of 40-70%, under a 10/14 h light/dark cycle.

CEU molecular imaging. Mice were anesthetized with inhaled isoflurane (1.5%). The jugular vein was cannulated for microbubble administration. Imaging of the proximal ascending aorta was performed with an ultrahigh frequency (25 MHz) mechanical sector imaging system. CEU was performed with Contrast Pulse Sequencing, which detects the nonlinear fundamental signal component for microbubbles. At each injection, images were acquired (MI 0.16) 8 min after intravenous injection of targeted or control microbubbles ($3x10^6$/ml; 2.2±1.7 μm) performed in random order. Microbubbles in the sector were then destroyed by increasing the mechanical index to 1.0 for 0.5 sec. Subsequent

post-destruction images were acquired at a mechanical index of 0.16. In order to test the specificity of Mb_{A1} to activated platelets on the endothelium, *in vivo* blocking experiments were performed with an additional group of 3 $ApoE^{-/-}$ mice at 32 weeks of age. CEU molecular imaging of platelets with Mb_{A1} and Mb_{ctrl} was performed in these mice before and after administration of 1.5 μg/g GpIbα antibody (cat. no. R300, Emfret Analytics GmbH & Co. KG) by intraperitoneal injection, which can result in 95% platelet immune depletion.

Image analysis. Signals from microbubbles were quantitatively estimated by commercially available software (Vevo 2100 imaging analysis software; FUJIFILM Visual Sonics, Inc.). During CEU imaging, 8 min after intravenous injection of microbubbles, the first 20 pre-destruction contrast frames were used to derive the total quantity of microbubbles, including retained and freely circulating microbubbles. To determine the signal from retained microbubbles alone, all microbubbles in the region of interest were destroyed and the subsequent 20 post-destruction contrast frames represented the freely circulating microbubbles. Therefore, the signal from targeted retained microbubbles was calculated by digitally subtracting 20 averaged post-destruction contrast frames from 20 averaged pre-destruction frames. Intensity was measured from a region-of-interest placed on the aorta arch.

Histology. After imaging, the 10% neutral formalin perfusion-fixed short-axis sections from the ascending aorta in $ApoE^{-/-}$ mice were evaluated in all study groups. Masson trichrome staining (11) was performed for assessment of plaque morphometry and the severity of atherosclerotic lesions. Immunohistochemistry for platelet expression was performed with a rabbit polyclonal primary antibody against GPIIb (cat. no. Ab63983; Abcam) and species-appropriate Alexa Fluor-594 secondary antibody (Invitrogen; Thermo Fisher Scientific, Inc.) was used.

Statistical analysis. Data were analyzed using SPSS (version 17.0; SPSS, Inc.), all parameter data were tested for normality and homogeneity of variance. The Shapiro Wilk test was used to verify whether continuous variables met the normal distribution, and all the data were presented as the mean ± SD. Comparisons of *in vitro* microbubble adhesion at different shear conditions were performed using one-way ANOVA method followed by Bonferroni multiple comparison tests. Independent t-tests were used to compare the number of attached microbubbles and the signal enhancements between Mb_{A1} and Mb_{ctrl}. Comparisons of the signal enhancements in the different age cohorts within the same animal group were made with one-way ANOVA and Bonferroni for multiple comparison tests. $P<0.05$ was considered to be statistically significant.

Results

Flow chamber activated platelets attachment studies

Preparation of PRP. PRP was prepared with a concentration of $399x10^9$/l. The platelet recovery rate was 167.65%, which exceeded 100%. Under microscopy, platelets with a high purity were seen on PRP smears stained with Wright Giemsa (Fig. S1A).

Platelet activation. Under the microscope, activated platelets were seen in a state of aggregation on the parallel plate culture dishes (Figs. S1B and S2A). Indirect immunofluorescence revealed a CD62 positive green fluorescent signal from activated platelets (Fig. S2B).

Flow chamber studies. Under light microscopy, activated platelets coating the parallel plate culture dishes were seen to be aggregated into irregular clusters (Fig. 1A and C). Under fluorescence microscopy, DiO labeled Mb_{A1} appeared selectively attached to activated platelet aggregates (Fig. 1B; green areas). However, DiI labeled Mb_{ctrl} (red areas), were sparse and not related to the aggregated platelets (Fig. 1D), which indicated nonspecific binding to the platelets. Across a range of shear stresses, attachment of Mb_{A1} to activated platelet aggregates was significantly higher than that of Mb_{ctrl} lacking a targeting ligand ($P<0.05$ at each shear stress; Fig. 2). With the shear stress increased from 2.0 to 8.0 dynes/cm^2, the number of attached Mb_{A1} remained constant ($P>0.05$; Fig. 2). There was no statistical difference ($P>0.05$) in the quantity of attached Mb_{ctrl} from 2.0 to 8.0 dynes/cm^2.

Molecular imaging of platelet adhesion. In $ApoE^{-/-}$ mice, CEU molecular imaging of the proximal ascending aorta detected selective signal enhancement from Mb_{A1} compared to Mb_{ctrl} at 8, 16 and 32 weeks of age (Fig. 3). Imaging signals from Mb_{A1} increased from 8 to 32 weeks of age ($P<0.05$). Signals from Mb_{ctrl} were low and similar between groups. In C57Bl/6 mice, there was no statistical difference in imaging signal between Mb_{ctrl} and Mb_{A1} (Fig. 3). After *in vivo* platelet immune depletion in 3 $ApoE^{-/-}$ mice at 32 weeks of age, the selective signal of Mb_{A1} decreased significantly ($P<0.05$), from 10.71 before blocking to 2.2 after blocking.

Immunohistochemistry. In $ApoE^{-/-}$ mice, the plaque lesions progressed from 8-32 weeks. There was mild intimal thickening in aorta sections at 8 weeks of age. Small but discrete fibrous plaques were seen at 16 weeks of age. At 32 weeks of age, large plaques with a lipid-rich core and a necros region were seen in all the sections, and these lesions tended to protrude into the aortic lumen (Fig. 4). Immunohistochemistry for GPIIb revealed the presence of platelets on the endothelial cell surface. In $ApoE^{-/-}$ mice, minimal and local GPIIb expression were present on the intimal surface of the aorta at 8 and 16 weeks of age (Fig. 4). With plaque progression, abundant GPIIb expression was detected on the intimal surface and in atherosclerotic lesions at 32 weeks of age (Fig. 4).

Discussion

Molecular imaging of inflammation with ultrasonography has been achieved by surface modification of microbubble contrast agents with ligands targeted to specific molecular and cellular events (12). Kaufmann *et al* (13). successfully applied vascular cell adhesion molecule-1 targeted microbubbles to detect vascular inflammatory responses in apolipoprotein E deficiency mice with atherosclerotic lesions. McCarty *et al* (14) used GPIbα antibody as a targeting moiety and noninvasive molecular imaging could detect activated vWF on the vascular endothelium, which further contributed to reveal an advanced

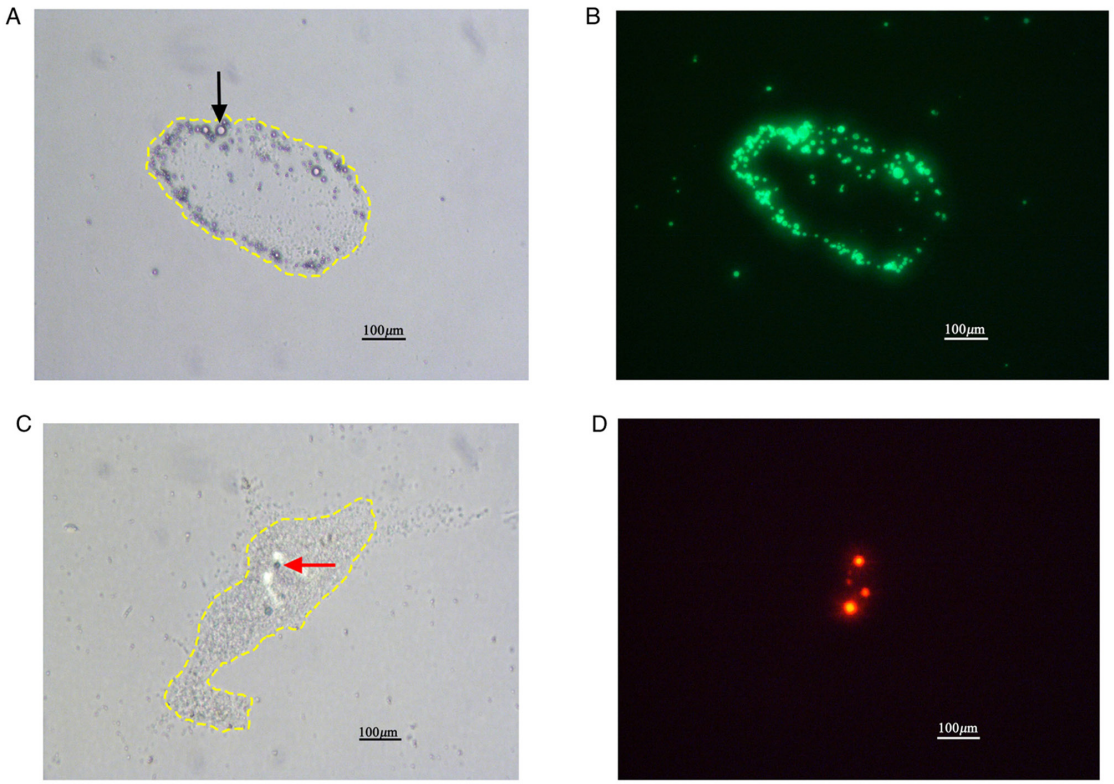

Figure 1. Attachment of Mb_{A1} or Mb_{ctrl} to platelet aggregates observed under an *in vitro* flow chamber at the shear stress of 8.0 dynes/cm^2. (A) Under light microscopy, activated platelets coating the parallel plate culture dishes aggregated into irregular clusters, circled by a yellow dashed line. A large amount of DiO labeled Mb_{A1} (black arrow) selectively attached to platelet aggregates, which was observed under (A) light microscopy and (B) fluorescence microscopy. Sparse DiI labeled Mb_{ctrl} (red arrow) was seen and not related to the aggregated platelets, which was confirmed under (C) light microscopy and (D) fluorescence microscopy, separately. Mb_{A1}, microbubbles with the vWF-A1 domain conjugated to the shell; Mb_{ctrl}; microbubbles with an isotype control conjugated to the shell; DiO, dioctadecyloxacarbocyanin; DiI, dioctadecyltetramethylindocarbocyanine.

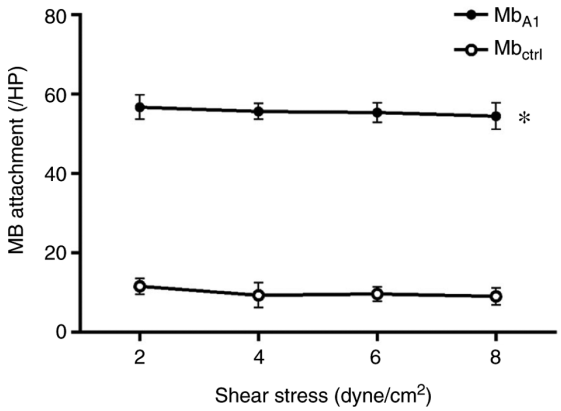

Figure 2. Mean ± SD number of microbubbles attached to platelet aggregates per high optical field in flow chamber studies. Attachment of Mb_{A1} to platelet aggregates was significantly greater than that of Mb_{ctrl} at each shear stress condition. With the shear stress increasing from 2.0 to 8.0 dynes/cm^2, the number of Mb_{A1} binding to platelet aggregates remained constant. Mb_{A1}, microbubbles with the vWF-A1 domain conjugated to the shell; Mb_{ctrl}; microbubbles with an isotype control conjugated to the shell. $^*P<0.05$ vs. Mb_{ctrl}.

prothrombotic and inflammatory phenotype in atherosclerotic disease.

It is widely accepted that platelets play a significant role in thromboembolic complications of advanced atherosclerotic lesions (15) and research attention is focused om platelet involvement in the formation of atherosclerotic lesions through platelet-endothelial interactions (16). In the present study, targeted CEU microbubbles bearing a recombinant vWF-A1 domain were prepared and their specific adhesion to activated platelets in a model flow chamber system and in a murine model of AS demonstrated. With these targeted microbubbles, the potent role of activated platelets in the process of AS can be further explored with CEU imaging.

Molecular imaging with CEU relies on the selective targeting and retention of acoustically active contrast agents at sites of disease (17). In the production of targeted microbubbles for molecular imaging, a typical strategy is to attach disease-specific ligands, including monoclonal antibodies, peptides, glycoproteins and other small molecules to the microbubble shell surface (18). A number of molecular imaging studies have focused on the attachment of monoclonal antibodies on the microbubbles because of their easy availability (19,20). However, there have been difficulties concerning the firm adhesion of microbubbles combined with antibodies under shear flow (21). The slow association kinetic properties and the high molecular weight of antibodies could be the reasons that reduce the capture efficiency on the target of interest. In previously studies on platelet targeting, targeted microbubbles were outfitted with monoclonal antibodies against GPIIb/IIIa (3,6). Unfortunately, the specific adhesion of these platelet targeted microbubbles was only observed under static conditions or dynamic flow conditions with low shear stress.

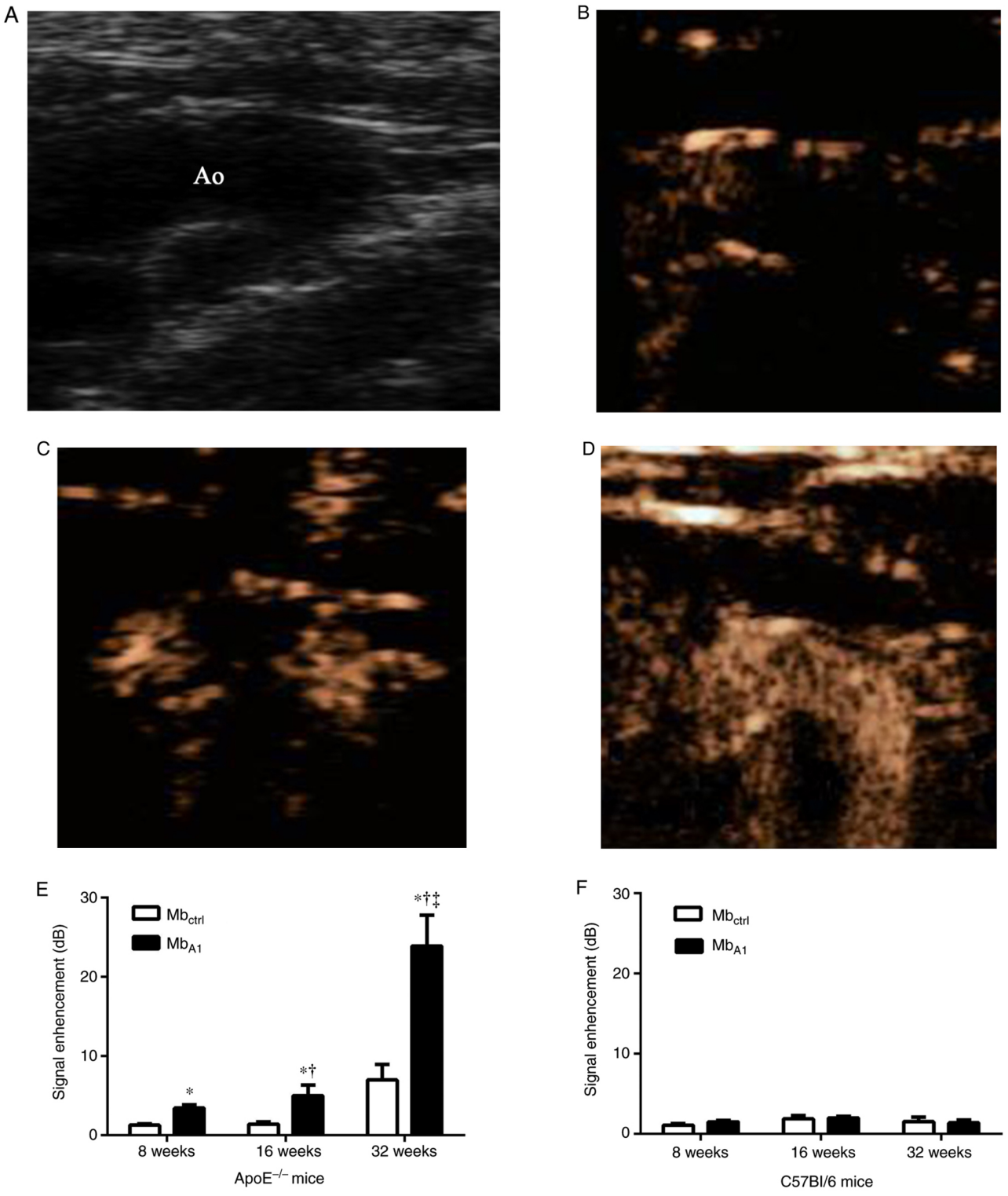

Figure 3. Examples of CEU molecular imaging of the proximal aortic arch at various ages with microbubbles targeted to platelets. (A) The proximal ascending aorta from ApoE$^{-/-}$ mice. Selective signal enhancements from Mb_{A1} at (B) 8, (C) 16 and (D) 32 weeks of age, separately. (E) In ApoE$^{-/-}$ mice, signal intensity from Mb_{A1} was stronger than that of Mb_{ctrl} at 8, 16, and 32 weeks of age, separately. Selective signal enhancement from Mb_{A1} can be detected at the early age of 8 weeks and increased from 8 to 32 weeks of age in ApoE$^{-/-}$ mice. Mb_{A1} signals in ApoE$^{-/-}$ mice were greater than that in C57Bl/6 mice at all time points. (F) In C57Bl/6 mice, there was no statistical difference in CEU molecular imaging signal between Mb_{ctrl} and Mb_{A1}. CEU, contrast-enhanced ultrasound; ApoE, apolipoprotein E; Mb_{A1}, microbubbles with the vWF-A1 domain conjugated to the shell; Mb_{ctrl}; microbubbles with an isotype control conjugated to the shell $^{*}P<0.05$ vs. Mb_{ctrl}, $^{\dagger}P<0.05$ vs. 8 weeks, $^{\ddagger}P<0.05$ vs. 16 weeks.

An increasing number of more studies have focused on preparation of targeted microbubbles with smaller peptide or peptide mimetic ligand molecules (22-24). Peptides, including polymeric sialyl Lewis X oligosaccharide derivatives (23) and short glycosulfopeptides (24), have been confirmed to provide efficient microbubble targeting even in fast flow. In the process

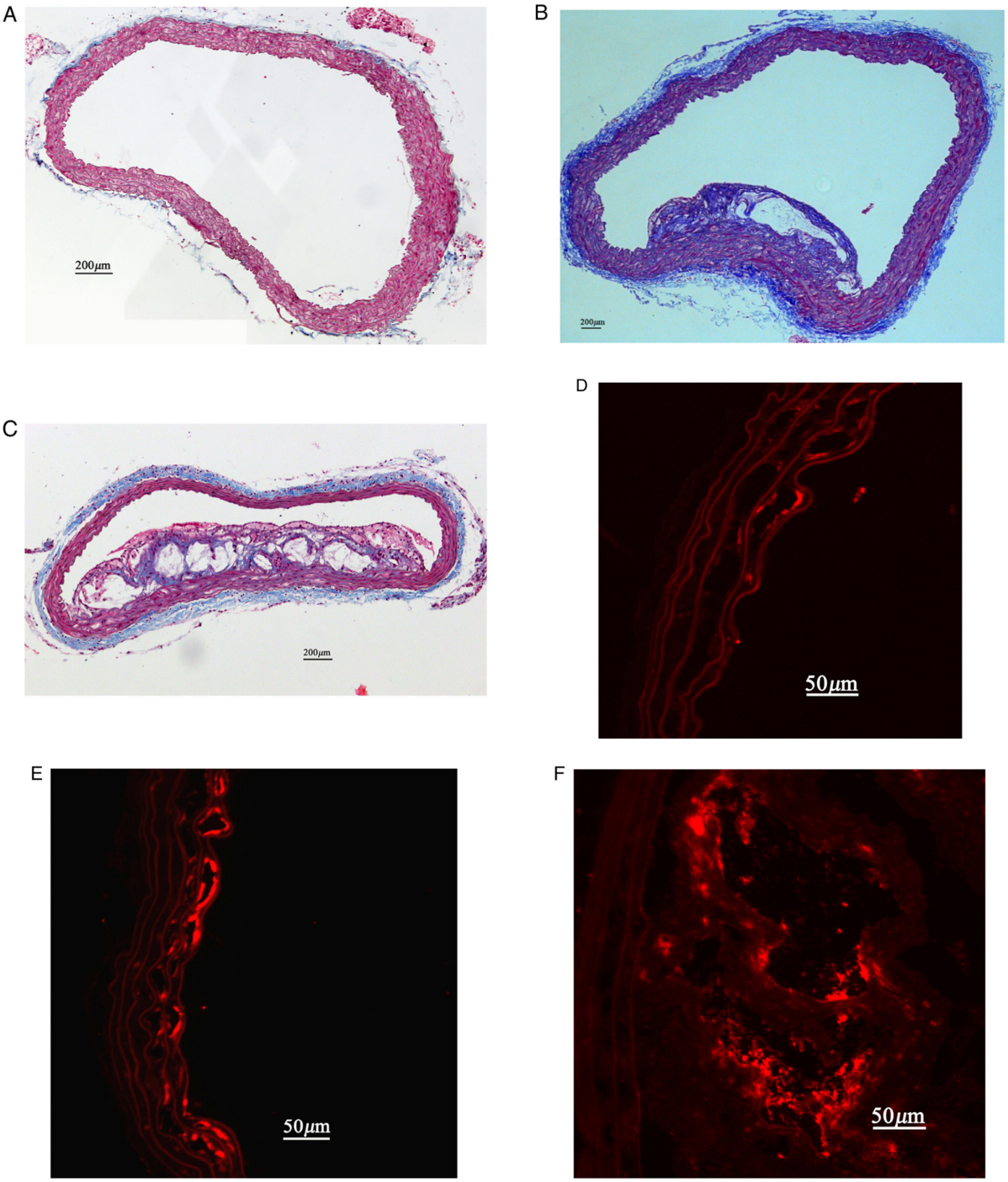

Figure 4. Masson trichrome and GPIIb staining of the proximal ascending aorta in ApoE$^{-/-}$ mice. (A) Image from ApoE$^{-/-}$ mice at 8 weeks of age showed mild intimal thickening in the endothelium. (B) Small but discrete fibrous plaques were detected at 16 weeks. (C) Large plaques with a lipid-rich core, necrotic region and inflammatory cell infiltration were detected at 32 weeks. GPIIb staining illustrated a difference in platelet accumulation in the different age groups of ApoE$^{-/-}$ mice at (D) 8 weeks of age, (E) 16 weeks of age and (F) 32 weeks of age. GP, glycoprotein; ApoE, apolipoproteinE.

of AS, platelet GPIbα plays a critical role in platelet adhesion and aggregation under high-shear conditions (7). GPIbα is a component of the GPIb-V-IX complex and initiates platelet adhesion by binding to collagen bound vWF (5). vWF is synthesized by endothelial cells and has multiple A, C and D type domains (25). In human blood flow, when the shear stress exceeds 400 dynes/cm^2, active A1 domains become exposed and can bind to GPIbα, acting as a hook for the capture of platelets and contributing to platelet adhesion under high vascular shear stress (26,27). The pivotal role of vWF-platelet interaction in mediating platelet adhesion under high-shear conditions indicated that the A1 domain of vWF could be a potential ligand used to prepare microbubbles targeted to platelets.

In the present study, a recombinant protein with an amino acid sequence corresponding to the A1 domain of vWF was used as the specific targeting ligand attached to the microbubble surface. The present study results confirmed the specific

attachment of Mb_{A1} to platelet aggregates under dynamic flow chamber conditions.

Differing from previous flow chamber studies, in which the specific attachment of targeted microbubbles conjugated to antibodies decreased with increasing shear stress, the present flow chamber experiment revealed that the number of Mb_{A1} binding to platelet aggregates remained constant when shear stress increased from 2.0 to 8.0 dynes/cm^2. The present results may provide insight into the high-strength interactions between platelets and vWF-A1 domain under dynamic flow conditions. In a study on a molten globule intermediate of the von Willebrand factor, the A1 domain firmly tethers platelets under shear flow. Tischer *et al* (28) suggested that the mean platelet pause times increased from ~0.75 sec at a shear stress of nearly 2.0 dynes/cm^2 to 0.9 sec at 8.0 dynes/cm^2, and then decreased again upon further increase of the shear stress. Pause times determined the average length of time a platelet was immobile, which has a complex dependence on the shear stress (28). With high shear stress exposing the vWF-A1 domain expressed on the endothelium, the active A1 domains become firmly bound to platelets. This behavior is referred to as a catch-slip interaction where the bond initially becomes weaker at low force, strengthens at intermediate forces and weakens again at higher forces (29,30), which could be the reason for the stable interactions between Mb_{A1} and platelets in the conditions of increasing shear stress from 2.0 to 8.0 dynes/cm^2. To the best of our knowledge, the targeted microbubbles bearing vWF-A1 domain prepared in the present study have higher affinities to platelets, which may produce favorable binding kinetics of microbubbles under high shear forces. Additionally, the vWF-A1 domain as a small molecular peptide is less immunogenic in humans, which may provide a better safety profile in future clinical application (31).

AS is a chronic inflammatory disease and various complex processes contribute to its pathophysiology and the development of the atherosclerotic plaque over decades (32,33). While it is now well established that platelets play a critical role in thrombotic complications of advanced AS, such as rupture of the vulnerable plaque, a growing experimental literature has established that platelets participate in the initiation of the atherogenic process through platelet-endothelium interaction (34). *In vivo* study of labeled platelets indicated that substantial numbers of platelets adhered to the carotid endothelium before the development of manifest atherosclerotic lesions in ApoE$^{-/-}$ mice (35). Consistent with these studies, using CEU molecular imaging in the present study, the presence of activated platelets on the vascular endothelium at the early lesion-prone stage of AS in *in vivo* experiments was confirmed. Moreover, there was also an age-dependent increase in selective signal enhancement from microbubbles bearing the A1 domain, indicating a relationship between the degree of platelet adhesion and disease severity. Platelets interacting with the endothelium may influence the development and progression of AS through a variety of mechanisms (36,37).

The intact nonactivated endothelium represents a natural barrier preventing platelet adhesion to the extracellular matrix. However, platelets can adhere directly to the intact but activated endothelial cell monolayer via GPIb/P-selectin or P-selectin glycoprotein ligand (PSGL)1/P-selectin (38). After contact between platelets and the endothelium has been established, platelets are activated and release proinflammatory cytokines and chemoattractants and express CD40 ligand to further induce the proatherogenic phenotype of endothelial cells (39,40). In this manner, adherent platelets enhance the recruitment of leukocytes, progenitor cells and dendritic cells to the vascular wall and tissues in the process for AS (41). Platelets not only promote an inflammatory response in leukocytes and endothelial cells, but may also themselves respond to inflammatory mediators produced by these cells. Studies have demonstrated that the bidirectional interaction between platelets and leukocytes and endothelial cells involves both inflammatory and prothrombotic pathways, contributing to a pathogenic loop in AS and plaque destabilization (37,42). Our application of CEU molecular imaging to evaluate the biological process of activated platelets in AS not only contribute to understanding the inflammatory role of platelets in AS, also can be used to explore the effects of new anti-platelets therapy in preventing AS.

The present study had several limitations. Firstly, the selective attachment of targeted microbubbles to activated platelets was explored in a parallel plate chamber. However, the flow in parallel plate chamber may not accurately simulate hemodynamics in the vessel to assess the binding efficiency of microbubbles *in vivo*. Secondly, the specific attachment to activated platelets was not directly compared between microbubbles bearing the vWF-A1 domain and those bearing antibodies. However, in the flow chamber studies with targeted microbubbles conjugated to monoclonal antibodies, the specific attachment of the targeted microbubbles decreased with increasing shear stress. Thirdly, though CEU molecular imaging was used to assess the extent of activated platelets in the process of atherogenesis, the underlying mechanisms contributing to the inflammatory progress were not explored in the present study.

Acknowledgements

Not applicable.

Funding

This research was supported by grants from the National Science Foundation of China (grant no. 81371581) and from the Natural Science Foundation of Hubei Province in China (grant no. 2019CFB691).

Availability of data and materials

The datasets used and/or analyzed during the current study are available from the corresponding author on reasonable request.

Authors' contributions

YL, JT and HL designed the experiments and wrote the manuscript. JT, YW, RS, YZ and JZ performed experiments and analyzed data. YL, HL and YZ assessed all the raw data and confirmed its authenticity and legitimacy. All authors

discussed the results and reviewed and approved the final manuscript.

Ethics approval and consent to participate

All animal experimental procedures were approved by the Animal Care and Use Committee of Tongji Medical College, Huazhong University of Science and Technology (Wuhan, China). Experiments involving human tissues were approved by Tongji Hospital Ethics Committee and volunteers provided their informed consent.

Patient consent for publication

Not applicable.

Competing interests

The authors declare that they have no competing interests.

References

1. Lievens D and von Hundelshausen P: Platelets in atherosclerosis. Thromb Haemost106: 827-838, 2011.
2. Feinstein SB, Coll B, Staub D, Adam D, Schinkel AF, ten Cate FJ and Thomenius K: Contrast enhanced ultrasound imaging. J Nucl Cardiol 17: 106-115, 2010.
3. Mendolicchio GL and Ruggeri ZM: New perspectives on von Willebrand factor functions in hemostasis and thrombosis. Semin Hematol 42: 5-14, 2005.
4. Ruggeri ZM: Platelets in atherothrombosis. Nat Med 8: 1227-1234, 2002.
5. Theilmeier G, Michiels C, Spaepen E, Vreys I, Collen D, Vermylen J and Hoylaerts MF: Endothelial von Willebrand factor recruits platelets to atherosclerosis-prone sites in response to hypercholesterolemia. Blood 99: 4486-4493, 2002.
6. Kumar RA, Dong JF, Thaggard JA, Cruz MA, López JA and McIntire LV: Kinetics of GPIbalpha-vWF-A1 tether bond under flow: Effect of GPIbalpha mutations on the association and dissociation rates. Biophys J 85: 4099-4109, 2003.
7. Sun R, Tian J, Zhang J, Wang L, Guo J and Liu Y: Monitoring inflammation injuries in the progression of atherosclerosis with contrast enhanced ultrasound molecular imaging. PLoS One 12: e0186155, 2017.
8. Shim CY, Liu YN, Atkinson T, Xie A, Foster T, Davidson BP, Treible M, Qi Y, López JA, Munday A, *et al*: Molecular imaging of platelet-endothelial interactions and endothelial von Willebrand factor in early and mid-stage atherosclerosis. Circ Cardiovasc Imaging 8: e002765, 2015.
9. Dhurat R and Sukesh M: Principles and methods of preparation of platelet-rich plasma: A review and author's perspective. J Cutan Aesthet Surg 7: 189-197, 2014.
10. Dunning K and Safo AO: The ultimate Wright-Giemsa stain: 60 years in the making. Biotech Histochem 86: 69-75, 2011.
11. Gao M, Xin G, Qiu X, Wang Y and Liu G: Establishment of a rat model with diet-induced coronary atherosclerosis. J Biomed Res 31: 47-55, 2016.
12. Moccetti F, Weinkauf CC, Davidson BP, Belcik JT, Marinelli ER, Unger E and Lindner JR: Ultrasound molecular imaging of atherosclerosis using small-peptide targeting ligands against endothelial markers of inflammation and oxidative stress. Ultrasound Med Biol 44: 1155-1163, 2018.
13. Kaufmann BA, Sanders JM, Davis C, Xie A, Aldred P, Sarembock IJ and Lindner JR: Molecular imaging of inflammation in atherosclerosis with targeted ultrasound detection of vascular cell adhesion molecule-1. Circulation 116: 276-284, 2007.
14. McCarty OJ, Conley RB, Shentu W, Tormoen GW, Zha D, Xie A, Qi Y, Zhao Y, Carr C, Belcik T, *et al*: Molecular imaging of activated von Willebrand factor to detect high-risk atherosclerotic phenotype. JACC Cardiovasc Imaging 3: 947-955, 2010.
15. Coenen DM, Mastenbroek TG and Cosemans JMEM: Platelet interaction with activated endothelium: Mechanistic insights from microfluidics. Blood 130: 2819-2828, 2017.
16. Behm CZ, Kaufmann BA, Carr C, Lankford M, Sanders JM, Rose CE, Kaul S and Lindner JR: Molecular imaging of endothelial vascular cell adhesion molecule-1 expression and inflammatory cell recruitment during vasculogenesis and ischemia-mediated arteriogenesis. Circulation 117: 2902-2911, 2008.
17. Myrset AH, Fjerdingstad HB, Bendiksen R, Arbo BE, Bjerke RM, Johansen JH, Kulseth MA and Skurtveit R: Design and characterization of targeted ultrasound microbubbles for diagnostic use. Ultrasound Med Biol 37: 136-150, 2011.
18. Piedra M, Allroggen A and Lindner JR: Molecular imaging with targeted contrast ultrasound. Cerebrovasc Dis 27 (Suppl 2): 66-74, 2009.
19. von Zur Muhlen C, von Elverfeldt D, Choudhury RP, Ender J, Ahrens I, Schwarz M, Hennig J, Bode C and Peter K: Functionalized magnetic resonance contrast agent selectively binds to glycoprotein IIb/IIIa on activated human platelets under flow conditions and is detectable at clinically relevant field strengths. Mol Imaging 7: 59-67, 2008.
20. Yan F, Sun Y, Mao Y, Wu M, Deng Z, Li S, Liu X, Xue L and Zheng H: Ultrasound Molecular Imaging of Atherosclerosis for Early Diagnosis and Therapeutic Evaluation through Leucocyte-like Multiple Targeted Microbubbles. Theranostics 8: 1879-1891, 2018.
21. Guenther F, von zur Muhlen C, Ferrante EA, Grundmann S, Bode C and Klibanov AL: An ultrasound contrast agent targeted to P-selectin detects activated platelets at supra-arterial shear flow conditions. Invest Radiol 45: 586-591, 2010.
22. Pochon S, Tardy I, Bussat P, Bettinger T, Brochot J, von Wronski M, Passantino L and Schneider M: BR55: A lipopeptide-based VEGFR2-targeted ultrasound contrast agent for molecular imaging of angiogenesis. Invest Radiol 45: 89-95, 2010.
23. Klibanov AL, Rychak JJ, Yang WC, Alikhani S, Li B, Acton S, Lindner JR, Ley K and Kaul S: Targeted ultrasound contrast agent for molecular imaging of inflammation in high-shear flow. Contrast Media Mol Imaging 1: 259-266, 2006.
24. Rychak JJ, Li B, Acton ST, Leppänen A, Cummings RD, Ley K and Klibanov AL: Selectin ligands promote ultrasound contrast agent adhesion under shear flow. Mol Pharm 3: 516-524, 2006.
25. Ju L, Chen Y, Zhou F, Lu H, Cruz MA and Zhu C: Von Willebrand factor-A1 domain binds platelet glycoprotein Ibα in multiple states with distinctive force-dependent dissociation kinetics. Thromb Res 136: 606-612, 2015.
26. Ruggeri ZM, Orje JN, Habermann R, Federici AB and Reininger AJ: Activation-independent platelet adhesion and aggregation under elevated shear stress. Blood 108: 1903-1910, 2006.
27. Ruggeri ZM: Von Willebrand factor, platelets and endothelial cell interactions. J Thromb Haemost 1: 1335-1342, 2003.
28. Tischer A, Madde P, Blancas-Mejia LM and Auton M: A molten globule intermediate of the von Willebrand factor A1 domain firmly tethers platelets under shear flow. Proteins 82: 867-878, 2014.
29. Thomas W: Catch bonds in adhesion. Annu Rev Biomed Eng 10: 39-57, 2008.
30. Thomas WE, Vogel V and Sokurenko E: Biophysics of catch bonds. Annu Rev Biophys 37: 399-416, 2008.
31. Inaba Y and Lindner JR: Molecular imaging of disease with targeted contrast ultrasound imaging. Transl Res 159: 140-148, 2012.
32. Hansson GK: Atherosclerosis - an immune disease: The Anitschkov Lecture 2007. Atherosclerosis 202: 2-10, 2009.
33. Davis NE: Atherosclerosis--an inflammatory process. J Insur Med 37: 72-75, 2005.
34. Hamilos M, Petousis S and Parthenakis F: Interaction between platelets and endothelium: From pathophysiology to new therapeutic options. Cardiovasc Diagn Ther 8: 568-580, 2018.
35. Massberg S, Brand K, Grüner S, Page S, Müller E, Müller I, Bergmeier W, Richter T, Lorenz M, Konrad I, *et al*: A critical role of platelet adhesion in the initiation of atherosclerotic lesion formation. J Exp Med 196: 887-896, 2002.
36. Kim H and Conway EM: Platelets and Complement Cross-Talk in Early Atherogenesis. Front Cardiovasc Med 6: 131, 2019.
37. Bakogiannis C, Sachse M, Stamatelopoulos K and Stellos K: Platelet-derived chemokines in inflammation and atherosclerosis. Cytokine 122: 154157, 2019.
38. Schulz C, Schäfer A, Stolla M, Kerstan S, Lorenz M, von Brühl M-L, Schiemann M, Bauersachs J, Gloe T, Busch DH, *et al*: Chemokine Fractalkine Mediates Leukocyte Recruitment to Inflammatory Endothelial Cells in Flowing Whole Blood. Circulation 116: 764-773, 2007.

39. King SM, McNamee RA, Houng AK, Patel R, Brands M and Reed GL: Platelet dense-granule secretion plays a critical role in thrombosis and subsequent vascular remodeling in atherosclerotic mice. Circulation 120: 785-791, 2009.
40. Aidoudi S and Bikfalvi A: Interaction of PF4 (CXCL4) with the vasculature: A role in atherosclerosis and angiogenesis. Thromb Haemost 104: 941-948, 2010.
41. Alexandru N, Andrei E, Dragan E and Georgescu A: Interaction of platelets with endothelial progenitor cells in the experimental atherosclerosis: Role of transplanted endothelial progenitor cells and platelet microparticles. Biol Cell 107: 189-204, 2015.
42. Aukrust P, Halvorsen B, Ueland T, Michelsen AE, Skjelland M, Gullestad L, Yndestad A and Otterdal K: Activated platelets and atherosclerosis. Expert Rev Cardiovasc Ther 8: 1297-1307, 2010.